deletions exist in the repertoire of the normal subjects (*13*) and show a pattern of specific V_β deletion in retrovirally infected humans. In mice, some V_β clonotypes susceptible to clonal deletions mediated by endogenous superantigens cross-react with exogenous superantigens (*4*). Thus, elimination of these cells early in ontogenesis may prevent the adverse effects that might occur later in life if such antigens are encountered (*4*). However, the absence of somatically imposed V_β deletions suggests that this concept cannot be applied to humans. Hence, the evolutionary pressures that have favored the advantages of maintaining a large T cell repertoire in humans may be ultimately responsible for the devastating pathogenic effect of HIV infection.

In conclusion, our results lend support to the hypothesis that HIV-encoded proteins may deliver anergic signals to noninfected T cells through interactions with specific V_β sequences. The final proof of this model will require the identification and the molecular characterization of the HIV-encoded superantigens. Such a characterization may also aid in avoiding deleterious effects of candidate vaccines.

REFERENCES AND NOTES

1. M. M. Davis, *Annu. Rev. Immunol.* **3**, 537 (1985); R. K. Wilson, E. Lai, P. Concannon, R. K. Bart, L. E. Hood, *Immunol. Rev.* **101**, 149 (1988); J. L. Strominger, *Science* **244**, 943 (1989).
2. J. W. Kappler, U. Staerz, J. White, P. Marrack, *Nature* **332**, 35 (1988); H. R. MacDonald *et al.*, *J. Exp. Med.* **167**, 2005 (1988); J. Kappler *et al.*, *Science* **244**, 811 (1989); C. A. Janeway, Jr., *Cell* **63**, 659 (1990).
3. Y. Choi *et al.*, *Proc. Natl. Acad. Sci. U.S.A.* **86**, 8941 (1989).
4. P. Marrack and J. Kappler, *Science* **248**, 705 (1990).
5. P. J. Dyason, A. M. Knight, S. Fairchild, E. Simpson, K. Tomonari, *Nature* **349**, 531 (1991); W. N. Frankel, C. Rudy, J. M. Coffin, B. T. Huber, *ibid.*, p. 526; P. Marrack, E. Kushnir, J. Kappler, *ibid.*, p. 524; D. L. Woodland, M. P. Happ, K. J. Gollob, E. Palmer, *ibid.*, p. 529.
6. H. Acha-Orbea *et al.*, *Nature* **350**, 207 (1991); Y. Choi, J. W. Kappler, P. Marrack, *ibid.*, p. 203.
7. A. Cerny *et al.*, *J. Exp. Med.* **171**, 315 (1990); A. W. Hügin, M. S. Vacchio, H. C. Morse III, *Science* **252**, 424 (1991).
8. Primers for V_β used in this study: V_β1, GCACAACAGTTCCCTGACTTGCAC; V_β2, TCATCAACCATGCAAGCCTGACCT; V_β3, GTCTCTAGAGAGAAGAAGGAGCGC; V_β4, ACATATGAG AGTGGATTTGTCATT; V_β5.1, ATACTTCAGTGAGACACAGAGAAAC; V_β5.2, TTCCCTAACTATAGCTCTGAGCTG; V_β6, AGGCCTGAGGGATCCGTCTC; V_β7, CCTGAATGCCCCA ACAGCTCTC; V_β8, ATTTACTTTAACAACAACGTTCCG; V_β9, CCTAAATCTCCAGACAAAGCTCAC; V_β10, CTCCAAAAACTCATCCTGTACCTT; V_β11, TCAACAGTCTCCAGAATAAGGACG; V_β12, AAAGGAGAAGTCTCAGAT; V_β13.1, CAAGGAGAAGTCCCCAAT; V_β13.2, GGTGAGGGTACAACTGCC; V_β14, GTCTCTCGAAAAGAGAAGAGGAAT; V_β15, AGTGTCTCTCGACAGGCACAGGCT; V_β16, AAAGAGTCTAAACAGGATGAGTCC; V_β17, CAGATAGTAAATGACTTTCAG; V_β18, GATGAGTCAGGAATGCCAAAGGAA; V_β19, CAATGCCCCAAGAACGCACCCTGC; V_β20, AGCTCTGAGGTGCCCCAGAATCTC; C_β3′, GTGCACCTCCTTCCCATT; and C_β5′, GTCCTGTGTTTGAGCCATCAGAA.
9. Primers for V_α used in this study: V_α1, CTGAGGTGCAACTACTCA; V_α2, AGAGGGAGCCTTAGCCTCTCTCAA; V_α3, AATGCCACCATGAACTGCAGTTAC; V_α4, ACAAGCATTACTGTACTCCTA; V_α5, GGCCCTGAACATTCAGGA; V_α6, TGACCAGCAAAATGCAACAGAAGG; V_α7, AGGAGCCATTGTCCAGATAAA; V_α8, GCTTATTCAAACAGCGCCTCAGAC; V_α9, CAGAGAGTGACTCAGCCCGAGAAG; V_α10, ACCCAGCTGGTGGAGCAGAGCCCT; V_α11, AGAAAGCAAGGACCAAGTGTT; V_α12, CACAACCTAACTCAAGCGCAGACT; V_α13, CTCATCAACCTGTTTTACATTCCC; V_α14, GCAGCTTCCCTTCCAGCAAT; V_α15, AGAACCTGACTGCCCAGGAA; V_α16, CCTCCAGTTCCTTCTGAA; V_α17, CAGCAGGTGAAACAAAGTCCTCAA; V_α18, TGTCAGGCAATGACAAGG; V_α22, TACACAGCCACAGGATACCCTTCC; C_α3′, ATGTCTAGCACAGTTTTGTCTGTG; and C_α5′, ATATCCAGAACCCTGACCCTGCCG.
10. G. Mantero, A. Zonaro, P. Bertolo, D. Primi, *Clin. Chem.* (*Winston-Salem, N.C.*) **37**, 422 (1991).
11. C. Janeway, *Nature* **349**, 459 (1991).
12. A. Herman, G. Croteau, R.-R. Sekaly, J. Kappler, P. Marrack, *J. Exp. Med.* **172**, 709 (1990).
13. R. Baccala, D. H. Kono, S. Walker, R. S. Balderas, N. Theofilopoulos, *Proc. Natl. Acad. Sci. U.S.A.* **88**, 2908 (1991).
14. P. Chomczynski and N. Sacchi, *Anal. Biochem.* **162**, 156 (1987).
15. A. Sottini, L. Imberti, R. Gorla, R. Cattaneo, D. Primi, *Eur. J. Immunol.* **21**, 461 (1991).

16. Supported by Sorin Biomedical (Saluggia, Italy) and IV Progetto AIDS, Istituto Superiore di Sanità.

26 June 1991; accepted 10 September 1991

Structure of a Legume Lectin with an Ordered N-linked Carbohydrate in Complex with Lactose

BOAZ SHAANAN,* HALINA LIS, NATHAN SHARON

The three-dimensional structure of the lactose complex of the *Erythrina corallodendron* lectin (EcorL), a dimer of N-glycosylated subunits, was determined crystallographically and refined at 2.0 angstrom resolution to an *R* value of 0.19. The tertiary structure of the subunit is similar to that of other legume lectins, but interference by the bulky N-linked heptasaccharide, which is exceptionally well ordered in the crystal, forces the EcorL dimer into a drastically different quaternary structure. Only the galactose moiety of the lactose ligand resides within the combining site. The galactose moiety is oriented differently from ligands in the mannose-glucose specific legume lectins and is held by hydrophobic interactions with Ala^{88}, Tyr^{106}, Phe^{131}, and Ala^{218} and by seven hydrogen bonds, four of which are to the conserved Asp^{89}, Asn^{133}, and NH of Gly^{107}. The specificity of legume lectins toward the different C-4 epimers appears to be associated with extensive variations in the outline of the variable parts of the binding sites.

RECOGNITION OF COMPLEX CARBOhydrates by lectins (*1*) has been implicated in important biological processes such as protein targeting to cellular compartments (*2*), homing of leukocytes (*3*), and host-pathogen interactions (*1*). The readily available plant lectins (*4, 5*) have become a paradigm for protein-carbohydrate recognition at the cell surface because of their ability to detect subtle variations in carbohydrate structures found on proteins and lipids from various sources. Structures of several plant lectins specific for mannose-glucose (Man-Glc), *N*-acetylglucosamine (GlcNAc)–sialic acid, and complexes of these lectins with sugars have been determined by crystallographic methods (*6–10*).

We report the high-resolution crystal structure of the *Erythrina corallodendron* lectin (EcorL) (*11*), which is specific for galactose and its derivatives, in complex with lactose (*12*). This legume lectin is a dimer of a 30-kD glycosylated subunit, homologous to other lectins of the same family (*5*), with a plant-specific heptasaccharide Manα6(Manα3)(Xylβ2)Manβ4GlcNAcβ4(L-Fucα3)GlcNAcβ N-linked to Asn^{17} of each subunit (*13*) (Xyl, xylose, and Fuc, fucose). Each subunit contains Mn^{2+} and Ca^{2+}, which are essential for the lectin activity (*11*). Beyond aspects related to the basis of sugar-binding specificity of the legume lectins, this report deals with the effect of glycosylation on protein assembly as well as with the interactions that stabilize branched surface carbohydrates in a single conformation.

The crystals of the EcorL-lactose complex are monoclinic *C*2, with cell dimensions a = 84.40 Å, b = 73.05 Å, c = 71.40 Å, and β = 113.42°, and contain one monomer in the asymmetric unit (*14*). The structure was determined by molecular replacement (*15*) by using the known structures of concanavalin A [Con A; (*16, 17*)] and pea lectin [PL (*9*)] as models. The *R* value of the current model is 0.190 at 2.0 Å resolution (*15*).

B. Shaanan, Laboratory of Molecular Biology, National Institute of Diabetes and Digestive and Kidney Diseases, National Institutes of Health, Building 2, Bethesda, MD 20892.
H. Lis and N. Sharon, Department of Biophysics, The Weizmann Institute of Science, Rehovot 76100, Israel.

*To whom correspondence should be addressed.

The tertiary structure of the EcorL monomer is similar to that of Con A and PL; most of the variations are localized to regions of β loops (*18*). Superposition of an EcorL monomer on that of Con A (Fig. 1) reveals that EcorL has the potential to sustain most of the interactions essential for maintaining the canonical legume lectin dimer first observed in Con A (*9, 16*), particularly the conserved β-sheet–type hydrogen bonds between main-chain atoms of the strands adjacent to and related by the molecular twofold axis. However, physical interference by the bulky carbohydrate chain emanating from the glycosylation site at Asn^{17}, which is part of the canonical monomer-monomer interface of the legume lectin family (*9, 16*), forces the EcorL dimer into a drastically different quaternary structure (Fig. 1). Rather than forming the conserved 12-strand β sheet extending over twofold related monomers, the two monomers of EcorL dock to build an interface of a "handshake" type similar in its general shape to that of the contact between the variable heavy-chain and light-chain (V_H-V_L) domains in F_{ab} fragments (*19*) (Fig. 1). The novel dimer thus formed is the genuine molecular dimer of EcorL (*20*). It is stabilized by hydrophobic and polar interactions, with a surface area of 700 $Å^2$ per subunit buried at the interface, but is probably less favorable than the canonical dimer, in which 900 to 1100 $Å^2$ per subunit are buried at the dimer interface and which is further stabilized by the β-sheet–type hydrogen bonds (*21*). The extreme effect of glycosylation on the assembly of EcorL can be related to the modulation of protein-protein interactions by an exposed N-linked carbohydrate that has been noticed in studies of the influenza virus hemagglutinin (*22*).

Attempts to determine by crystallographic methods the detailed structure of carbohydrate units on glycoproteins have been hampered by the inherent mobility and chemical heterogeneity of the oligosaccharides (*23, 24*). In the crystal of EcorL the N-linked heptasaccharide is tethered by an intricate network of intra- and intermolecular hydrogen bonds and as a result all of the seven monosaccharides are seen with exceptional clarity in the electron density map (Fig. 2A). The branched carbohydrate projects out from Asn^{17}, which is the last residue of a β turn connecting strands from the two main antiparallel β sheets characteristic of the legume lectins (*9, 16*). It adopts an extended conformation, with the β1 → 4 linked GlcNAc (NAG14 in Fig. 2B) and the terminal trimannoside unit roughly coplanar and nearly perpendicular to the mean plane of the first, N-linked GlcNAc (N-NAG in Fig. 2B). The latter monosaccharide and its

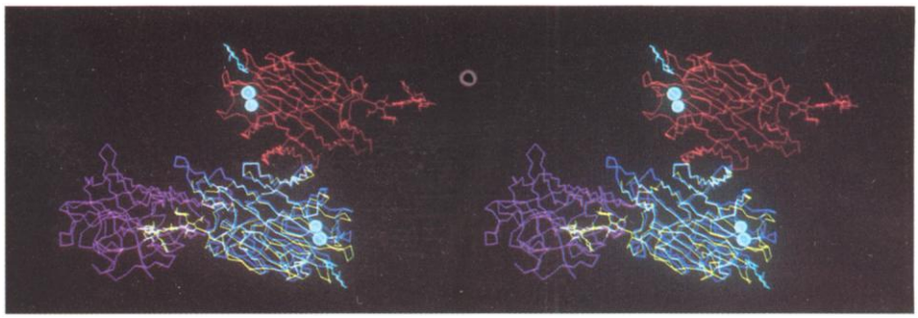

Fig. 1. The relation between the canonical dimer of the legume lectin family and that of EcorL (stereo). An EcorL monomer (yellow) is superimposed (*18*) on one monomer of the canonical dimer (two Con A monomers, blue and purple). The N-linked carbohydrate of EcorL penetrates ~17 Å into the second Con A monomer. The EcorL dimer (viewed down its twofold axis) is formed by interaction with another monomer (red) through three strands on the opposite side of the β sheet (metal ions and lactose ligand of EcorL shown in light blue).

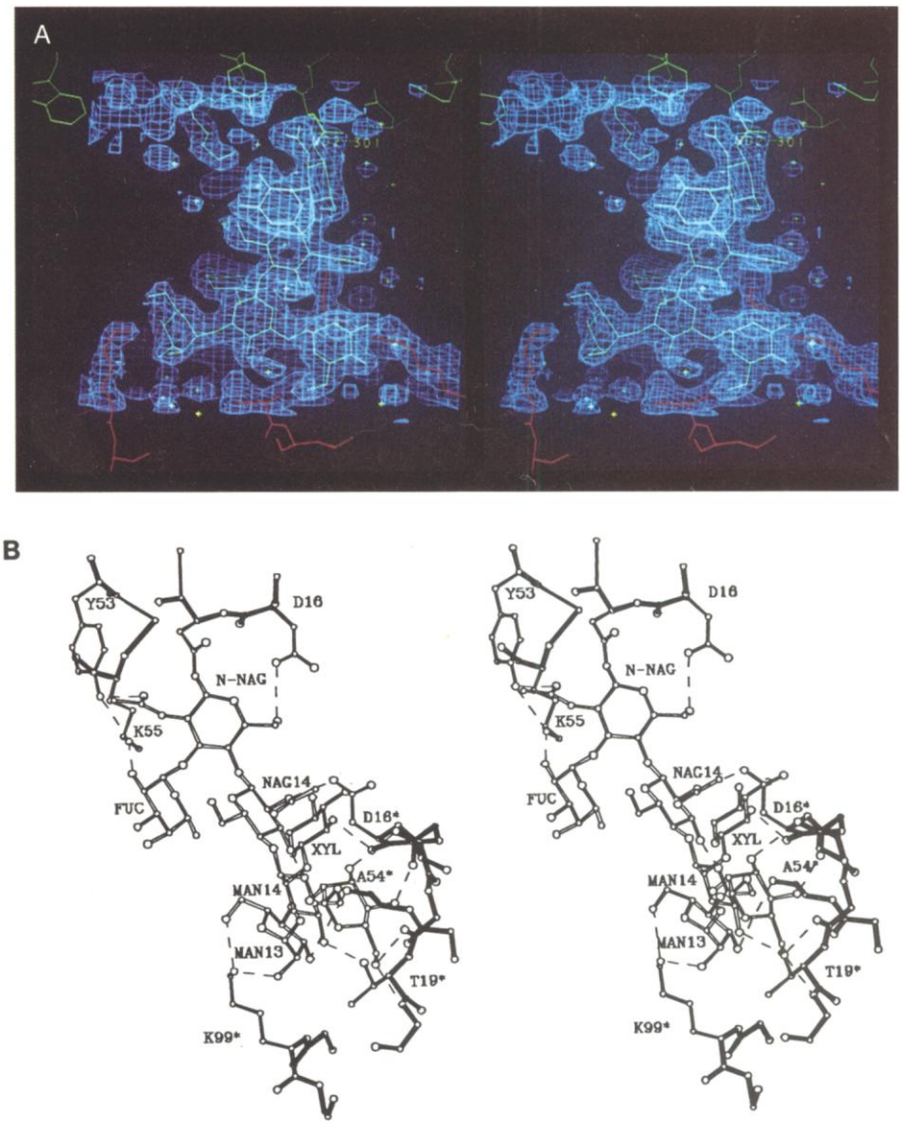

Fig. 2. The N-linked carbohydrate in EcorL (stereo). (**A**) $2F_o - F_c$ map (contoured at 1σ) with the protein molecule (light green; glycosylation site marked as ND2 301), the symmetry-related molecule (red), and water molecules (crosses). The fucose partially covers the β1 → 4GlcNAc, and the xylose is in the back. (**B**) The network of hydrogen bonds (dashed lines) stabilizing the N-linked carbohydrate (empty bonds; water molecules omitted for clarity). One letter code (*29*) and a sequence number for shown protein residues (full bonds); asterisks indicate symmetry-related residues.

1 → 3 linked L-fucose are held tightly by hydrogen bonds to side-chain atoms of Asp^{16}, Tyr^{53}, and Lys^{55} of the parent protein molecule, while the other saccharides, that is, the β1 → 4 GlcNAc, the trimannoside unit, and the xylose, form nine hydrogen bonds to main-chain and side-chain atoms on three separate β turns in the twofold related molecule [Fig. 2B (*20*)]. Discrete water molecules surround the monosaccharides in regions not in direct contact with the protein (Fig. 2A). Despite their relative proximity, there are no direct interactions between the two symmetry-related N-linked carbohydrate chains (*20*).

The EcorL structure accentuates the capability of proteins to force convergence to a particular conformer out of the vast, although somewhat restricted (*25*), ensemble of conformations accessible to exposed oligosaccharides, provided that the overall dynamic structure of the latter fits the contacting protein environment. Although the "frozen" conformation of the N-linked carbohydrate in the EcorL crystal is selected during the crystallization process by fortuitous interactions between the terminal saccharides and a complementary surface presented by a symmetry-related molecule, all of the dihedral angles associated with the glycosidic bonds of the heptasaccharide, except for the φ/ψ angles of the Man1 → 6 branch, fall within the angular range deduced from solution studies on similar or identical oligosaccharides (*25, 26*) (Table 1). In the EcorL crystal the flexible Man1 → 6 branch adopts an ω = −67° conformation about the C-5–C-6 bond, which differs from the conformation observed in (*26*) but was observed in other studies (Table 1) (*24, 25, 27*) with φ/ψ angles that optimize the interactions with the protein.

As in other legume lectins, the combining site of EcorL is a shallow depression on the protein surface that shares residues with the calcium binding site that is essential for sugar binding (*6–9, 16, 17*). The galactose moiety is well resolved in the electron density map of the EcorL-lactose complex, whereas the glucose, which resides mostly outside the binding pocket, is barely detectable beyond the glycosidic bond (Fig. 3A). Hydrophobic interactions with Ala^{88}, Tyr^{106}, Phe^{131}, and Ala^{218}, as well as seven cooperative hydrogen bonds (*28*) to protein atoms and to a bound water, hold the galactose in the combining site. Four hydrogen bonds are from the galactose 3-OH and 4-OH to Oδ2 of Asp^{89}, Nε2 of Asn^{133}, NH of Gly^{107}, and Oδ1 of Asp^{89}, which, along with the hydrophobic side chains of Ala^{88} and Phe^{131}, occupy similar relative positions in the combining sites of other legume lectins and constitute the framework necessary for binding sugars (*4*) (Figs. 3B and 4). Two additional hydrogen bonds are between 4-OH and NH of Ala^{218}, whose relative position in the binding pocket appears to vary somewhat between the legume lectins (Ala^{211} in PL and Leu^{99} in Con A; Figs. 3B and 4) and between 6-OH and Nε2 of Gln^{219} (Glu^{212} in PL and Tyr^{100} in Con A; Fig. 3B). The 6-OH is also hydrogen bonded to a water molecule that is bound tightly to the main-chain O of Leu^{86} (Figs. 3B and 4; see legend to Fig. 3B for hydrogen-bond distances between the ligand and protein atoms).

However, in EcorL, and presumably in other galactose-binding legume lectins (*10*), the orientation of the hexose ring with respect to the framework for ligand binding differs from the orientation observed in complexes of glucose-mannose specific lectins, probably as a result of the different stereoelectronic effects associated with the C-4 configuration of the ligands. The galactose is rotated in the combining site so that,

Table 1. Comparison of φ/ψ dihedral angles of the N-linked carbohydrate in the EcorL crystal and solution.

Linkage	φ/ψ (degrees)	
	Crystal	Solution*
L-Fucα(1 → 3)GlcNAc	45/19	45/30
GlcNAcβ(1 → 4)GlcNAc	47/11	50/10
Manβ(1 → 4)GlcNAc	41/−37†	60/0
Xylβ(1 → 2)Man	45/19	45/30
Manα(1 → 6)Man	−62/76‡	−40/170§
Manα(1 → 3)Man	5/−154	−15/−160

*The φ/ψ values in solution are based on studies of the bromelain hexasaccharide, which lacks the α1 → 3 Man (*26*). The last entry is from a study of the heptasaccharide of *Erythrina cristagalli* (*25*), which is identical to that of EcorL. See (*25*) and (*26*) for definitions of the dihedral angles ω, φ, and ψ. †Within 3 kcal/mol from the solution conformation (*26*). ‡ω = −67°. §ω = 180°.

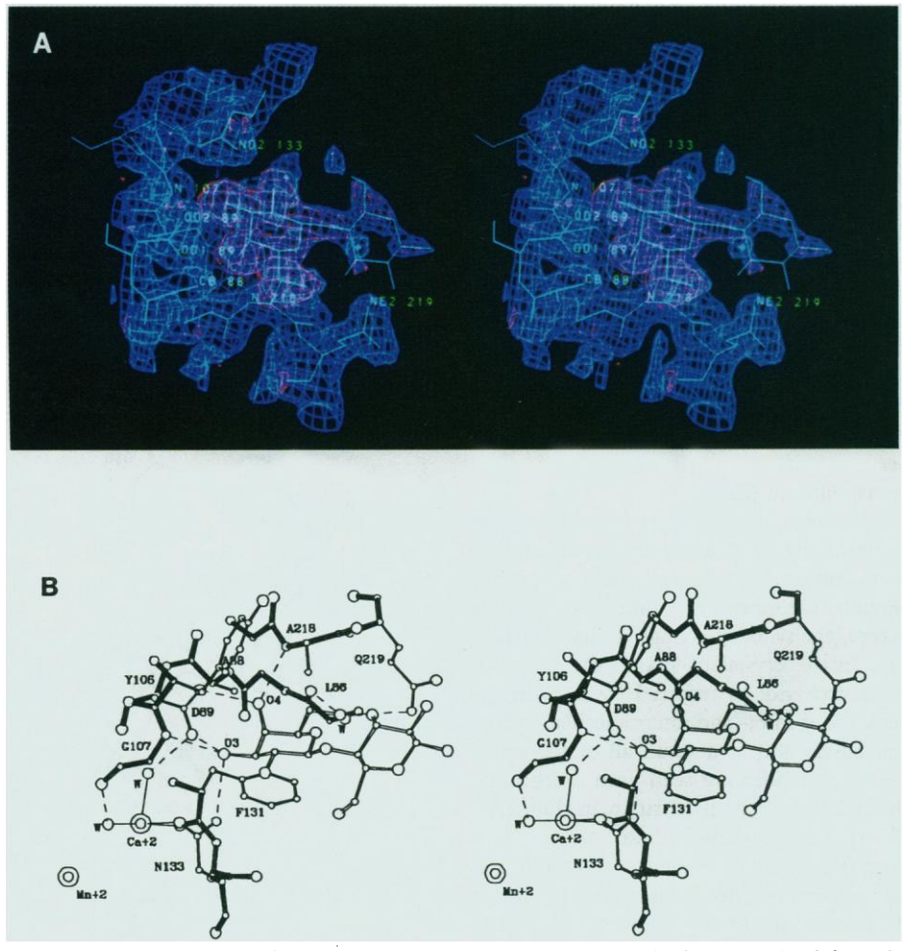

Fig. 3. The combining site of EcorL (stereo). (**A**) $F_o - F_c$ map (purple; lactose omitted from the model) superimposed on $2F_o - F_c$ map (both maps contoured at 1σ). (**B**) The hydrogen bonds (dashed lines) and hydrophobic residues stabilizing the ligand (empty bonds) in the combining site of the EcorL-lactose complex. Only the galactose (3-OH and 4-OH as O3 and O4, respectively) makes hydrogen bonds to protein residues (full lines; marked as in Fig. 2B). Hydrogen-bond distances: 3-OH to Oδ2 of Asp^{89}, to NH of Gly^{107}, and to Nε2 of Asn^{133} are 2.8, 2.9, and 3.1 Å, respectively; 4-OH to Oδ1 of Asp^{89} and NH of Ala^{218} are 2.8 and 2.9 Å, respectively; and 6-OH to Nε2 of Gln^{219}, 3.1 Å. Note the *cis*-peptide bond between Ala^{88} and Asp^{89} (*4, 6, 9*).

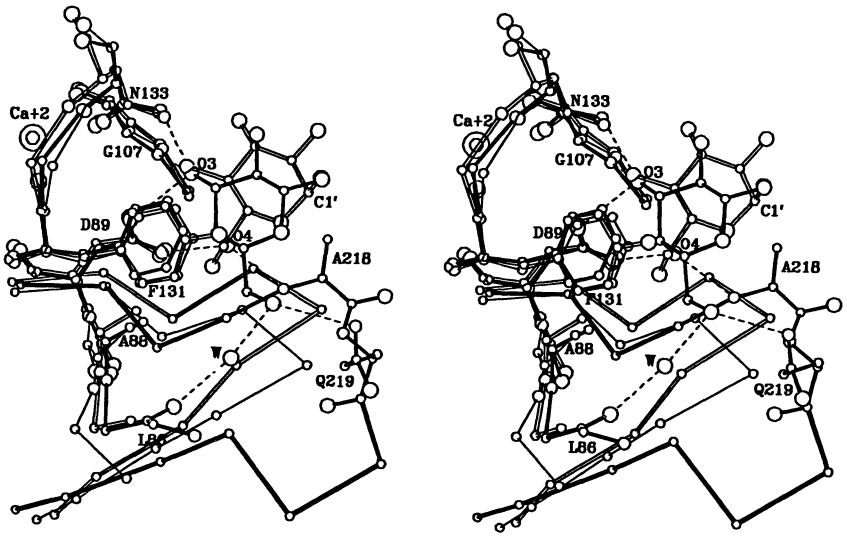

Fig. 4. Comparison (stereo) of the combining sites of EcorL (full bonds), Con A (empty bonds), and PL (single line). Residues were superimposed by using the transformation matrices derived in (*30*). Shown are EcorL residues in contact with the ligand and the corresponding residues in Con A and PL in the framework for ligand binding (other residues in the Cα tracing), the galactose (full bonds; 3-OH and 4-OH marked) with hydrogen bonds (dashed lines) to EcorL residues and the glucose (empty bonds, C-1 marked as C1′) as positioned in the Con A combining site (7). The C-1 (glucose)–Cβ(Ala^{218}) distance is 2.2 Å. The residues of the framework for ligand binding (Ala^{88}, Asp^{89}, Phe^{131}, Asn^{133}, and the NH of Gly^{107} in EcorL) overlap within error with the equivalent residues in PL (Ala^{80}, Asp^{81}, Phe^{123}, Asn^{125}, and Gly^{99}) and Con A (Ala^{207}, Asp^{208}, Tyr^{12}, Asn^{14}, and Arg^{228}, the latter shown without its side chain).

for example, its 3-OH and 4-OH groups make hydrogen bonds to Nε2 of Asn^{133} and Oδ1 of Asp^{89}, respectively, whereas the glucose-mannose forms hydrogen bonds to the equivalent protein atoms through 4-OH and 6-OH (*7, 8*). The 6-OH of the galactose is accommodated in EcorL by a radically different trace of the β turn constituting the more structurally variable edge of the combining site around residues Ala^{218} and Gln^{219} and opposite the conserved framework (Figs. 3B and 4). Furthermore, model building (Fig. 4) suggests that steric hindrance by the side chain of Ala^{218} in EcorL plays a major role in discriminating against binding of glucose-mannose as it prevents optimal positioning of ligands with an equatorial 4-OH [such as glucose; (*11*)].

Thus, the adjustable topology of the combining sites of the legume lectins enables them to optimally align the specific ligands with respect to the conserved constellation of residues that are involved directly in hydrogen bonds and hydrophobic interactions with the bound sugar (Ala^{88}, Asp^{89}, Gly^{107}, Phe^{131}, and Asn^{133} in EcorL; Fig. 4). However, although subtle variations in the shape and size of residues lining the combining sites can account for variations in ligand affinity among the glucose-mannose specific lectins (*4*), the EcorL structure suggests that extensive differences in the outline of the variable parts of the binding pockets are associated with specificity toward the different C-4 epimers.

REFERENCES AND NOTES

1. N. Sharon and H. Lis, *Science* **246**, 227 (1989).
2. G. Ashwell and A. G. Morell, *Adv. Enzymol.* **41**, 99 (1974); G. Ashwell and J. Harford, *Annu. Rev. Biochem.* **51**, 531 (1982).
3. B. K. Brandley, S. J. Swiedler, P. W. Robbins, *Cell* **63**, 861 (1990); T. A. Springer and L. A. Laskey, *Nature* **349**, 196 (1991); S. D. Rosen, *Am. J. Respir. Mol. Cell Biol.* **3**, 397 (1990), and references therein.
4. G. N. Reeke, Jr., and J. W. Becker, *Curr. Top. Microbiol. Immunol.* **139**, 35 (1988); J. W. Becker and G. N. Reeke, Jr., *Trans. Am. Crystallogr. Assoc.* **25**, 37 (1991).
5. N. Sharon and H. Lis, *FASEB J.* **4**, 3198 (1990).
6. G. M. Edelman *et al.*, *Proc. Natl. Acad. Sci. U.S.A.* **69**, 2580 (1972); K. D. Hardman and C. F. Ainsworth, *Biochemistry* **11**, 2910 (1972); G. N. Reeke, Jr., and J. W. Becker, *Science* **234**, 1108 (1986); Y. Bourne *et al.*, *J. Mol. Biol.* **214**, 571 (1990); C. Wright, *ibid.* **218**, 635 (1990).
7. Z. Derewenda *et al.*, *EMBO J.* **8**, 2189 (1989).
8. Y. Bourne *et al.*, *Proteins* **8**, 365 (1990).
9. H. M. Einspahr, E. H. Parks, K. Suguna, E. Subramanian, F. L. Suddath, *J. Biol. Chem.* **261**, 16518 (1986).
10. Preliminary results of a crystallographic study at 2.8 Å resolution of the *Griffonia simplicifolia* lectin IV complexed with Lewis^b tetrasaccharide in which the lectin binds the β-D-galactose of the ligand have been described in L. T. Delbaere *et al.*, *Can. J. Chem.* **68**, 1116 (1990); *Trans. Am. Crystallogr. Assoc.* **25**, 51 (1991).
11. H. Lis, F. J. Joubert, N. Sharon, *Phytochemistry* **24**, 2803 (1985); R. Adar, M. Richardson, H. Lis, N. Sharon, *FEBS Lett.* **257**, 81 (1989); R. Arango, S. Rozenblatt, N. Sharon, *ibid.* **264**, 169 (1990).
12. The association constant for binding lactose to EcorL is $1.15 \times 10^3\ M^{-1}$ (F. G. Loontiens, H. Lis, N. Sharon, unpublished results) based on measurements as described in H. De Boeck, F. G. Loontiens, H. Lis, N. Sharon, *Arch. Biochem. Biophys.* **234**, 297 (1984).
13. D. Ashford *et al.*, *Eur. J. Biochem.* **166**, 311 (1987).
14. Crystals of the complex were grown by equilibrating hanging drops of 15 μl containing 6 mg/ml protein, 10 mM lactose, 15% 2,4-methylpentane-diol (MPD), 50 mM Hepes, pH 7.0, and 0.01% sodium azide against reservoirs containing 30% MPD and 100 mM Hepes. Diffraction data to 2.0 Å resolution were collected on a Siemens area detector, mounted on a Rigaku RU-200 source, and processed by using the programs XENGEN [A. J. Howard *et al.*, *J. Appl. Crystallogr.* **20**, 383 (1987)], XDS [(W. Kabsch, *ibid.* **21**, 916 (1988)], and the CCP4 package (SERC Daresbury Laboratory, United Kingdom). Altogether, 123,808 observations from two crystals were merged and averaged to yield 26,597 independent reflections (99.5% of all possible reflections to 2.0 Å resolution) with an overall R_{sym} of 0.052 [$R_{sym} = \Sigma_h\Sigma_i|\langle I(\mathbf{h})\rangle - I(\mathbf{h})_i|/\Sigma_h\Sigma_i(\mathbf{h})_i$].
15. The models of Con A and PL were superimposed by using a rotation function. Structure factors for the probe were calculated by Fourier inversion of the concatenated coordinate sets of the two models after superposition according to the rotation function. This combined model served as a probe for the rotation and translation search with the programs MERLOT [P. M. D. Fitzgerald, *J. Appl. Crystallogr.* **21**, 273 (1988)] and BRUTE [M. Fujinaga and R. J. Read, *ibid.* **20**, 517 (1987)]. The correct solutions of the rotation and translation functions were the highest peaks (9.2 and 4.5 σ above the mean, respectively), which yielded a model with an R value [$R = \Sigma_h|F_o(\mathbf{h}) - F_c(\mathbf{h})|/\Sigma_h F_o(\mathbf{h})$] of 0.42 for all of the reflections in the range from 3.0 to 10 Å. This model was extensively rebuilt and refined by using the programs XPLOR [A. T. Brünger, in *Crystallographic Computing 4. Techniques and New Technologies*, N. W. Isaacs and M. R. Taylor, Eds. (Oxford Univ. Press, Oxford, 1988), pp. 126–140] and PROLSQ [W. A. Hendrickson and J. H. Konnert, in *Computing in Crystallography*, R. Diamond, S. Ramaseshan, K. Venkatesan, Eds. (Indian Academy of Sciences, Bangalore, 1980), pp. 13.01–13.23]. The N-linked carbohydrate, lactose ligand, and 100 water molecules were built into difference maps after the refinement had converged to an R value of 0.22. The current R value is 0.190 for all of the reflections between 2.0 and 6.0 Å, with 0.018 Å and 3° root-mean-square (rms) deviation from ideality for bond lengths and bond angles, respectively. All but three residues fall within the allowed regions of the Ramachandran plot.
16. J. W. Becker, G. N. Reeke, Jr., J. I. Wang, B. A. Cunningham, G. M. Edelman, *J. Biol. Chem.* **250**, 1513 (1975); G. N. Reeke, Jr., J. W. Becker, G. M. Edelman, *ibid.*, p. 1525.
17. K. D. Hardman, R. C. Agarwal, M. J. Freiser, *J. Mol. Biol.* **157**, 69 (1982).
18. Superposition of the main-chain atoms of EcorL on those of Con A and PL results in an root square (rms) values of 1.53 and 1.06 Å, respectively. For superposition of atoms in the β strand the values are 0.63 and 0.80 Å for EcorL-Con A and EcorL-PL, respectively.
19. D. R. Davies, E. A. Padlan, D. M. Segal, *Contemp. Top. Mol. Immunol.* **4**, 127 (1975); L. M. Amzel and R. J. Poljak, *Annu. Rev. Biochem.* **48**, 961 (1979).
20. The molecular dimer of EcorL is generated by two monomers related by the $0,y,\frac{1}{2}$ twofold axis. The hexagonal ($P6_5$) form of EcorL [M. A. Saper, H. Lis, N. Sharon, B. Shaanan, *J. Mol. Biol.* **193**, 823 (1987)] contains the whole dimer in the asymmetric unit, as confirmed by a molecular replacement study with the dimer of the *C*2 form described here as a probe and which, after rigid-body refinement, yielded an R value of 0.31 for all of the data between 3.5 and 6.0 Å (B. Shaanan, unpublished results). The intermolecular network of hydrogen bonds stabilizing the N-linked heptasaccharide forms between two independent monomers related by the $0,y,0$ twofold axis.
21. A detailed description of the interface and the structure will be published elsewhere.
22. J. J. Skehel *et al.*, *Proc. Natl. Acad. Sci. U.S.A.* **81**, 1779 (1984).
23. I. A. Wilson, J. J. Skehel, D. C. Wiley, *Nature* **289**, 363 (1981); B. J. Sutton and D. C. Phillips, *Biochem. Soc. Trans.* **11**, 130 (1983); J. N. Varghese, W. G. Laver, P. M. Colman, *Nature* **303**, 35 (1983); D. Suck, C. Oefner, W. Kabsch, *EMBO J.* **3**, 2423 (1984); R. L. Williams, S. M. Green, A. McPherson, *J. Biol. Chem.* **262**, 16020 (1987); W. Bode,

E. Meyer, Jr., J. C. Powers, *Biochemistry* **28**, 1951 (1989); W. I. Weis, A. T. Brünger, J. J. Skehel, D. C. Wiley, *J. Mol. Biol.* **212**, 737 (1990).
24. J. Deisenhofer, *Biochemistry* **20**, 2361 (1981).
25. S. Homans, R. A. Dwek, T. W. Rademacher, *ibid.* **26**, 6553 (1987); *ibid.*, p. 6571.
26. J. B. Bouwstra *et al.*, *Eur. J. Biochem.* **190**, 113 (1990).
27. J. P. Brisson and J. Carver, *Biochemistry* **22**, 3680 (1983).
28. F. A. Quiocho, *Annu. Rev. Biochem.* **55**, 287 (1986); *Philos. Trans. R. Soc. London Ser. B* **326**, 341 (1990).
29. Abbreviations for the amino acid residues are: A, Ala; C, Cys; D, Asp; E, Glu; F, Phe; G, Gly; H, His; I, Ile; K, Lys; L, Leu; M, Met; N, Asn; P, Pro; Q, Gln; R, Arg; S, Ser; T, Thr; V, Val; W, Trp; and Y, Tyr.
30. In order to compare the topologies of the combining sites of EcorL, Con A, and PL, the Mn^{2+}, Ca^{2+}, and 16 atoms of conserved residues and water molecules in the coordination spheres of the metals in the three lectins were superimposed [from EcorL: Oδ1 and Oδ2 of Asp^{89}, Asp^{129}, and Asp^{136}, Oε1 and Oε2 of Glu^{127}, O of Phe^{131}, Oδ1 and Nδ2 of Asn^{133}, Nε2 of His^{142}, and water molecules 801, 807, 808, and 809; the equivalent residues in Con A (*17*) are Asp^{208}, Asp^{10}, Asp^{19}, Glu^{8}, Tyr^{12}, Asn^{14}, His^{24}, and the four water molecules in W3.239 and in PL (entry 2LTN in the Brookhaven Protein Data Bank) are Asp^{81}, Asp^{121}, Asp^{129}, Glu^{119}, Phe^{123}, Asn^{125}, His^{136}, and water molecules A417, A422, A456, and A657]. The rms values for the superposition of the EcorL atoms on those of Con A and PL were 0.34 and 0.27 Å, respectively.
31. Thanks are due to D. R. Davies for interest in the project and support, E. A. Padlan, G. H. Cohen, and C. C. Hyde for useful suggestions, K. D. Hardman for coordinates of Con A, D. Ashford and C. Edge for the initial model of the N-linked heptasaccharide, R. Adar for the primary sequence, and S. Haalman and M. Laschver for technical assistance. Supported in part by grants to N.S. from BSF (3727), from BARD (IS-1636-89), and the Leo and Julia Forchheimer Center for Molecular Genetics at The Weizmann Institute. The coordinates of the current model have been deposited in the Brookhaven Protein Data Bank (entry 1LTE). The model on the cover was generated by the program Ribbon 2.0 [M. Carson, *J. Mol. Graphics* **5**, 103 (1987)] and rendered by AVS software (Stardent Computer Inc.).

27 June 1991; accepted 4 September 1991

A Phosphorylation Site in the Na^+ Channel Required for Modulation by Protein Kinase C

JAMES W. WEST, RANDAL NUMANN, BRIAN J. MURPHY, TODD SCHEUER, WILLIAM A. CATTERALL

Voltage-gated sodium channels are responsible for generation of action potentials in excitable cells. Activation of protein kinase C slows inactivation of sodium channels and reduces peak sodium currents. Phosphorylation of a single residue, serine 1506, that is located in the conserved intracellular loop between domains III and IV and is involved in inactivation of the sodium channel, is required for both modulatory effects. Mutant sodium channels lacking this phosphorylation site have normal functional properties in unstimulated cells but do not respond to activation of protein kinase C. Phosphorylation of this conserved site in sodium channel α subunits may regulate electrical activity in a wide range of excitable cells.

VOLTAGE-SENSITIVE Na^+ CHANnels are responsible for the initiation and propagation of the action potential and therefore play a crucial role in neuronal excitability (*1*). The Na^+ channel isolated from rat brain is a heterotrimeric protein consisting of a 260-kD α subunit and 30- to 40-kD β_1 and β_2 subunits (*2*). Expression of the α subunit is sufficient for formation of functional Na^+ channels in *Xenopus* oocytes (*3*) or mammalian cells (*4*). Four rat brain Na^+ channel subtypes have been defined by cloning and sequencing (*5–7*). Types II and IIA are the predominant Na^+ channel α-subunit subtypes expressed in adult rat forebrain (*8, 9*). Physiological modulation of these Na^+ channels would lead to significant changes in neuronal excitability in the brain. Protein kinase C (PKC) modulates the activity of many ion channels (*10*) and is known to phosphorylate the α subunit of the Na^+ channel in rat brain (*11*). Activation of PKC in *Xenopus* oocytes expressing brain Na^+ channels decreases peak Na^+ current (*12*). We have recently found that activation of PKC in rat brain neurons or in transfected Chinese hamster ovary (CHO) cells expressing type IIA Na^+ channels (CNaIIA-1) (*13*) causes rapid and reversible slowing of Na^+ channel inactivation and reduction of peak Na^+ current (*14*).

Both slowing of inactivation and reduction of peak Na^+ current were recorded in every cell-attached patch (*15*) from CNaIIA-1 cells (*16*) treated with 40 to 75 μM 1-oleoyl-2-acetyl-*sn*-glycerol (OAG). To quantify the slowing of inactivation without fitting to a specific model, we normalized the peak Na^+ currents, measured their integral, and expressed it as percent of untreated controls. Treating the cells with 40 to 50 μM OAG reduced the peak Na^+ current to 33 ± 7% of control and increased the normalized peak current integral to 206 ± 68% of control (SEM, n = 16); treating the cells with 65 to 75 μM OAG further reduced the peak current to 6 ± 0.3% of control (SEM, n = 6). PKC phosphorylation can almost completely inhibit Na^+ currents in these CNaIIA-1 cells.

The intracellular loop between domains III and IV (Fig. 1) plays a critical role in Na^+ channel inactivation (*17, 18*). The presence of a consensus PKC phosphorylation site (*19*) centered at Ser^{1506} in this intracellular loop led us to consider whether phosphorylation of Ser^{1506} might be involved in modulation of Na^+ channel activity by PKC. The synthetic peptide SP19 (*17*) (Fig. 1) represents a portion of the intracellular loop between homologous domains III and IV and contains the putative PKC site Lys-Lys-Leu-Gly-Ser-Lys-Lys. Peptide SP19 was rapidly phosphorylated by purified PKC (*20*) in vitro in the presence of diolein and phosphatidylserine (240 nmol/min per milligram of enzyme) but not by adenosine 3′,5′-monophosphate (cAMP)–dependent protein kinase (<2 nmol/min per milligram

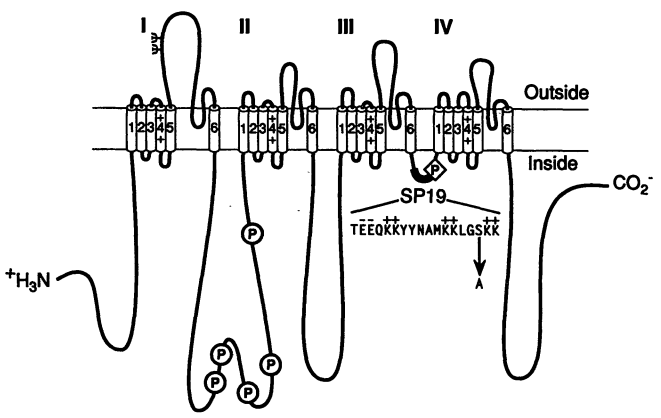

Fig. 1. The transmembrane folding model of the Na^+ channel α subunit with experimentally determined cAMP-dependent protein kinase phosphorylation sites (P enclosed in a circle) and the putative PKC phosphorylation site (P enclosed in a diamond). The single-letter amino acid code of the primary sequence of the SP19 peptide in the intracellular loop between homologous domains III and IV of the type IIA Na^+ channel α subunit (*6*) is illustrated. The arrow indicates the position of the oligonucleotide-directed mutation of Ser^{1506} to alanine. Abbreviations for the amino acid residues are as follows: A, Ala; E, Glu; M, Met; N, Asn; Q, Gln; T, Thr; and Y, Tyr.

Department of Pharmacology, University of Washington, Seattle, WA 98195.